

Preliminary study on the osseointegration effects of contactless automated implant cavity preparation via femtosecond laser ablation

SHANSHAN LIANG,^{1,2,3,4,5} JIANQIAO ZHENG,^{1,2,3,4,5} AND FUSONG YUAN^{1,2,3,4,5,*}

¹Center of Digital Dentistry/Department of Prosthodontics, Peking University School and Hospital of Stomatology, Beijing 100081, China

²National Center of Stomatology & National Clinical Research Center for Oral Diseases, Beijing 100081, China

³National Engineering Laboratory for Digital and Material Technology of Stomatology, Beijing 100081, China

⁴Beijing Key Laboratory of Digital Stomatology, Beijing 100081, China

⁵NHC Research Center of Engineering and Technology for Computerized Dentistry, Beijing 100081, China
*yuanfusong@bjmu.edu.cn

Abstract: Microrobots were used to control the femtosecond laser ablation of bone tissues to prepare implant cavities for dental implant surgery. The method was optimized through depth-of-cut experiments of ex vivo rabbit femurs, and the optimized method was used to prepare implant cavities on the left femurs of eight live rabbits. A power of 10 W and a scanning rate of 4000 mm/s were found to be optimal. After seven days of osteoinduction, the expression of collagen type I was significantly higher in the experimental group than in the control group (manually drilled implant cavities). The bone–implant contacts of the experimental group at 4 and 8 weeks were 9.65% and 23.08%, respectively.

© 2021 Optica Publishing Group under the terms of the [Optica Open Access Publishing Agreement](#)

1. Introduction

Dental implants are artificial roots placed in the alveolar bone as replacements for missing teeth [1]. Dental implants can be restored and loaded immediately after implantation or at a later time [2]. Dental implant therapy does not involve tooth preparation procedures on the remaining healthy natural teeth, and it significantly improves mastication [3]. Furthermore, dental implants are aesthetically pleasing and conducive for the retention of local soft and hard tissues. Thus, dental implant therapy is often the optimal choice of treatment for patients with missing teeth [4]. The key to the success of this procedure is in the preparation of implant cavities, which is traditionally performed by drilling holes at the implant positions using a dental drill. After the drilling positions are located, a pilot bur is used to drill through the cortical bone, and the drill is gradually enlarged until the desired cavity size is achieved [5,6].

The conventional approach of implant cavity preparation strongly relies on the experience and skill of the dental practitioner. Consequently, the position and direction of the implant cavity are easily affected by subjective factors, such as practitioner skill, individual patient variations (e.g., small mouth opening), and the emotional state of the practitioner. The adverse consequences resulting from failures during this process can include implant failure [7], damage to the adjacent dental roots [8], severe damage to the mandibular nerve [9], damage to the submental artery [9], and fatal hemorrhages in extreme cases [10].

Dental implant surgery has become less invasive, increasingly precise, and safer in recent times owing to advancements in dental implant technology [11]. Surgical guidance techniques are now being used to improve the precision of implant cavity preparation [12]. The most common among these techniques include static surgical templates [13] and dynamic surgical guidance;

these techniques are useful for determining the correct position of each implant while improving the placement precision [14]. However, implant precision may still be affected by errors in template design and fabrication or imprecisions in the guidance system [11]. Furthermore, such guidance systems can eliminate neither the intrinsic limitations of conventional implant burs nor the influence of subjective factors on the precision and safety of dental implant surgery [15].

Intelligent robotics is a burgeoning trend that is shaping the future of medicine [16]. Numerous studies have been conducted to ascertain whether robotics can be used to address the difficulties of dental implant surgery [17–20]. However, most robot-controlled implant preparation systems reported in the literature exclusively use specialized low-speed implant burs [17,18] that require multiple burs for the drilling process and are encumbered by limited access to the posterior mandible. Furthermore, physical contact (cutting, compression, and friction) between the bur and alveolar bone inevitably generates mechanical vibrations and heat [21,22]. This heat in turn increases the temperature of the bur and its surrounding osseous tissue. High temperatures can harm the osseous tissues and hinder osseointegration [23,24].

Femtosecond lasers are extremely precise and have low laser-induced damage thresholds because they produce low heat and do not generate impact waves [25]; furthermore, they can be precisely controlled in all three coordinate axes, which allows the precise removal of material without heat damage. Extensive studies have been conducted on the use of femtosecond lasers for medical applications. These lasers are being widely used in scientific research, medical, and industrial applications [26–31].

A few studies have demonstrated the use of femtosecond lasers for ablating osseous tissues [32–37]. For instance, Lim et al. used femtosecond laser ablation to fabricate micropillars on bovine cortical bone, proving that femtosecond lasers can ablate osseous tissues [34]. McCaughey et al. performed stapedotomy by femtosecond laser ablation and compared their results to those obtained using an Er:YAG laser. They observed that femtosecond laser ablation was more precise and that the heat damage caused to the surrounding tissues was negligible [35]. Lo et al. used a femtosecond laser to perform osteotomies on mouse skulls; they found that laser osteotomy produced less tissue damage and better healing rates than mechanical osteotomies at 2-, 4-, and 6-week evaluations post-surgery [36]. Su et al. investigated the use of pulsed lasers as alternatives to microfracture surgery and found that femtosecond laser systems could be used for cartilage removal without damaging the underlying bones [37].

Currently, there are no reports on the use of robot-controlled femtosecond lasers for automated implant cavity preparation in dental surgery. To address this limitation, we constructed an automated and contactless implant cavity preparation system by combining a femtosecond laser with robotics technology. This work represents a preliminary investigation of the steps included in automated implant cavity preparation using the proposed robot-controlled femtosecond laser system as well as the effects of the procedure on osseointegration.

2. Methods

2.1. Preparation of *ex vivo* rabbit femurs

Three *ex vivo* femurs were retrieved from New Zealand rabbits euthanized via anesthetic overdose at the animal experimentation room of the Peking University Stomatological Hospital on the same day as their euthanization. This study has been approved by the Biomedical Ethics Committee of Peking University (No. LA2021061). All surface cartilage tissues were removed from the femurs, which were then washed in physiological saline. The less even sides of the femurs were wrapped in silicone rubber to form flat surfaces, while the flatter sides were polished with 800-, 1000-, and 2000-grit wet sandpapers. The polished femurs were stored in a freezer at -20 °C.

2.2. Laser ablation and surface roughness measurements

Laser ablations were conducted with a computer-controlled femtosecond laser (Tangerine, Amplitude system, France) at 1030 nm with a pulse frequency of 200 kHz, pulse energy of 50 μJ , focused beam diameter of 80 μm , and fluence of 1 J/cm^2 , along with a self-developed mini robot (focal length: 170 mm, scanning rate of the two-dimensional (2D) galvanometer scanner: 0–7000 mm/s, repeatability: $<8 \mu\text{rad}$, minimum step along the z-axis: 0.1 μm). The ablation power of the femtosecond laser was varied at 5, 10, and 15 W with a scanning rate of either 4000 or 6000 mm/s, thereby producing six distinct experimental conditions.

The to-be-cut surfaces of the rabbit femurs were placed along the focal plane of the galvanometer scanner. A micrometer (Mitutoyo, Japan) with a precision of 0.01 mm was used to adjust the position of the stage with respect to the direction of incidence of the laser beam, such that the to-be-cut surfaces were perpendicular to the principal beam axis and located exactly on the laser focal plane. The femtosecond laser was then used to cut out three-stepped concentric circles with progressively widening diameters on the femur bones (Fig. 1). A three-dimensional (3D) laser scanning microscope (Keyence, VK-X200, Japan) was used to measure five random longitudinal cross-sections of each concentric circle. The height of each step was also measured, and 15 height measurements were averaged to obtain one sample. Thus, 18 samples were obtained from the six experimental groups, and the depth-of-cut of each experimental group (corresponding to a certain combination of laser parameters) was obtained by averaging the three samples in that group. The 3D laser scanning microscope was also used to measure the surface roughnesses of the cuts on the rabbit femurs (Fig. 2). The surface roughness values at five randomly selected 100 $\mu\text{m} \times 100 \mu\text{m}$ grids were averaged.



Fig. 1. Concentric circles with steps of varying depths on an ex vivo rabbit femur.

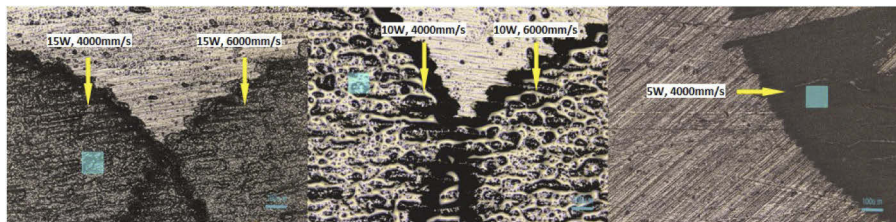


Fig. 2. Surface roughness measurements on an ex vivo rabbit femur using a 3D laser scanning microscope.

2.3. Parameter optimization for automated implant cavity preparation

The ex vivo rabbit femurs were polished with wet sandpaper, as noted previously. The polished femurs were then affixed to a stage using silicone rubber, and the stage was adjusted such that it was located on the cutting plane along the focal plane of the laser. Implant cavities were ablated using the femtosecond laser in a layer-wise manner. The parameters of the femtosecond laser system were configured according to the depths of the cuts. The femurs were then cut in half along their longitudinal axes by wire electrical discharge machining to facilitate the visual inspection of the implant cavities and bone marrow.

2.4. Evaluation of implant cavity preparation and postoperative osteogenic activity

The robot-controlled femtosecond laser ablation system was configured for the optimal parameters and used to automatically prepare a 3 mm × 3 mm implant cavity on the left femur of eight 2.5 kg New Zealand rabbits. Another 3 mm × 3 mm implant cavity was prepared on the right femurs of these rabbits using conventional implant drilling burs with standard operating parameters.

After four of the rabbits were euthanized, their femurs were removed and placed in Dulbecco's Modified Eagle Medium (DMEM) (with 5% penicillin and 5% streptomycin), and the samples were moved to a biosafety cabinet. The left femurs of these rabbits were placed in a petri dish and washed three times with phosphate-buffered saline (PBS) (with 5% penicillin and 5% streptomycin). All cartilage tissue on the femoral surfaces were scraped off in the PBS. Next, the ends of the femurs were removed, and a 2 mL syringe was used to draw the growth medium and dispense the cells inside the femur into a petri dish containing 2 mL DMEM (with 10% fetal bovine serum and 1% penicillin–streptomycin). The DMEM was first exchanged after half a day and then re-exchanged on the third day. Subsequently, it was exchanged once in every three days. The right femurs, which had manually drilled implant cavities, were used as the controls.

All of the aforementioned procedures were repeated for the right femur. Once the cells were subcultured for seven days to facilitate osteogenic differentiation, western blotting was used to measure the expression of collagen type I, Runx2, P-alkaline (ALP), SP7, and osteopontin proteins in the eight cell-protein samples. The final results were analyzed using the SPSS statistical software program (SPSS 19.0, SPSS Inc., USA). The influence of osseointegration between different methods for implant cavity preparation was investigated using one-way analysis of variance.

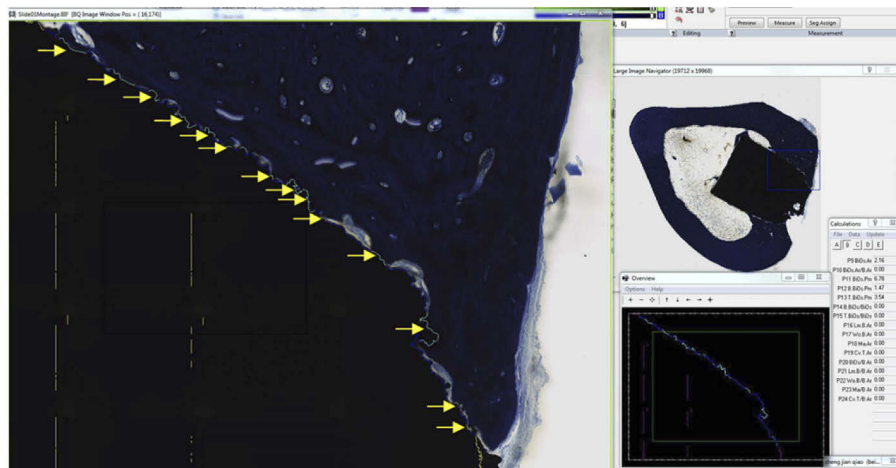


Fig. 3. Measurement of BIC using BIOQUANT OSTEO (green lines indicated by the yellow arrows are areas where the bone is fully intact).

In the four remaining rabbits, 3 mm × 3 mm simulated titanium roots were implanted into the cavities on the left and right legs. These titanium roots were fabricated by additive manufacturing using direct metal laser melting machines (Concept Laser, Mlab cusing R, Germany) and titanium powder (rematitan CL alloy, 99.3% pure, 50 μm Ti₆Al₄V powder, Concept Laser, Germany), with subsequent sterilization in an autoclave. Two of the rabbits were randomly euthanized at 4 weeks, and the remaining two were euthanized at 8 weeks. Hard tissue sections were prepared from all animals, and the bone–implant contact (BIC, where BIC% = area of contact between the implant and new bone/length of the implant in the cortical bone) was assessed in each section using BIOQUANT OSTEO. The differences between the proposed cavity preparation and conventional methods were consequently analyzed in terms of the BIC (Fig. 3).

3. Results

Table 1 shows the depths of the cuts measured by the 3D laser scanning microscope after femtosecond laser ablation for the six distinct parameter combinations. Table 2 shows the surface roughness of the cuts from femtosecond laser ablation for five of the parameter combinations. The results of visual inspection of the implant cavities prepared by femtosecond laser ablation and their longitudinal cross-sections are shown in Fig. 4 and 5 and Table 3.



Fig. 4. Implant cavities prepared with different combinations of laser-cutting parameters.

3.1. Results of parameter optimization

The results in Table 1 show that femtosecond lasers with powers of 5 W, 10 W, and 15 W can ablate rabbit cortical bone. The depth of the ablation increases with power and decreases with scanning rate; at 5 W and 6000 mm/s, no significant cutting marks were observed. Thus, the 5 W/6000 mm/s setting combination was not used for surface roughness measurements or implant cavity preparations. From the surface roughness measurements, it is observed that the roughness increases with laser power. The roughness associated with a power of 10 W and a scanning rate

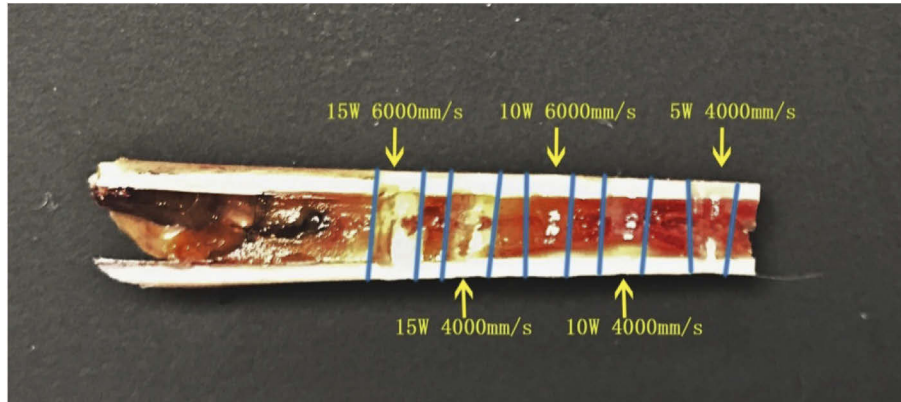


Fig. 5. Longitudinal cross-sections of the prepared implant cavities.

Table 1. Cut depths in ex vivo rabbit femurs with different combinations of femtosecond laser parameters

| Power (W) | Number of scans | Scanning rate (mm/s) | Depth-of-cut (μm) |
|-----------|-----------------|----------------------|--------------------------------|
| 15 | 5 | 4000 | 42 |
| 15 | 5 | 6000 | 33 |
| 10 | 5 | 4000 | 36 |
| 10 | 5 | 6000 | 30 |
| 5 | 20 | 4000 | 18 |
| 5 | 20 | 6000 | - |

Table 2. Surface roughnesses of ex vivo rabbit femurs ablation with different combinations of femtosecond laser parameters

| Power (W) | Scanning rate (mm/s) | Roughness $R_a \pm \text{std. dev}$ (μm) |
|-----------|----------------------|---|
| 15 | 6000 | 3.57 ± 0.32 |
| 15 | 4000 | 3.64 ± 0.43 |
| 10 | 6000 | 3.18 ± 0.47 |
| 10 | 4000 | 2.95 ± 0.52 |
| 5 | 4000 | 2.08 ± 0.38 |

Table 3. Visual inspection of the cortical bone after femtosecond laser ablation with different parameter combinations

| Power (W) | Scanning rate (mm/s) | Number of passes | Visual inspection |
|-----------|----------------------|------------------|-------------------------------------|
| 15 | 6000 | 100 | Carbonized bone marrow |
| 15 | 4000 | 100 | Damaged bone marrow |
| 10 | 6000 | 100 | No carbonization in the bone marrow |
| 10 | 4000 | 100 | No carbonization in the bone marrow |
| 5 | 4000 | 100 | No carbonization in the bone marrow |

of 4000 mm/s was reasonably low. During the preparation of the implant cavities in the ex vivo femurs, it was observed that a power of 15 W caused the marrow to change color (Fig. 5); no such changes were observed for the 10 or 5 W cases. The longitudinal cross-sections of the implant cavities also showed that lower power settings increase implant taper. Based on these results, it was concluded that the optimal parameters for automated implant cavity preparation by robot-controlled femtosecond laser ablation are a power of 10 W and a scanning rate of 4000 mm/s. These parameters were used in the subsequent implant cavity preparations for live animal experiments.

3.2. Western blot analysis

Figure 6 illustrates the differences between the control and experimental groups in terms of the expression of osteogenic proteins by the bone marrow mesenchymal stem cells (BMSCs) in an osteoinductive environment. The glyceraldehyde 3-phosphate dehydrogenase (GAPDH) gene expression was identical in all groups. One-way analysis of variance indicates that the expression of collagen type I was significantly higher in the experimental group than in the control group after 7 days of osteoinduction ($P < 0.05$); no significant differences were observed in the expressions of the other proteins ($P > 0.05$). Therefore, it may be concluded that femtosecond laser cutting promotes the expression of osteogenic proteins by the BMSCs to a certain extent.

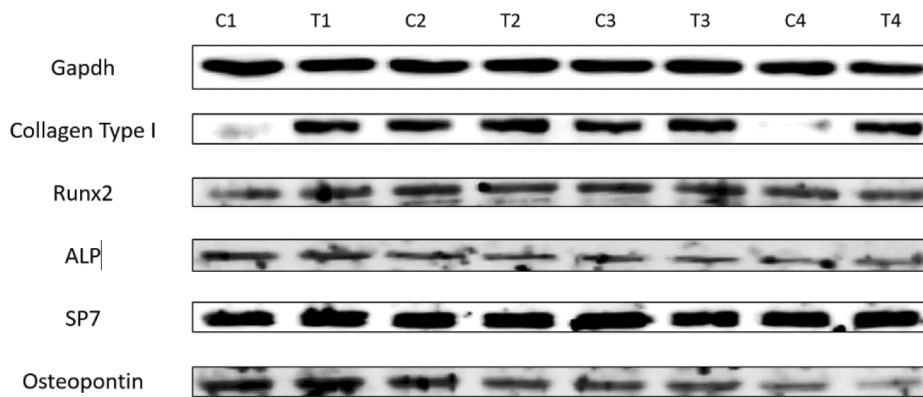


Fig. 6. Expressions of GAPDH as well as collagen type I, Runx2, P-alkaline, SP7, and osteopontin proteins in the BMSCs of the control and treated groups based on western blot analysis.

3.3. Analysis of hard tissue sections

Figure 7 shows the bone histological sections of the rabbits that were euthanized at 4 and 8 weeks after the implantation of the titanium implants. In the experimental group, the growth of new bone tissues at the titanium implants and inner edges of the implant cavities increased rapidly over time, and their BICs at 4 and 8 weeks were 9.65% and 23.08%, respectively. The same trends were observed in the control group, for which the BICs at 4 and 8 weeks were 9.55% and 20.93%, respectively.

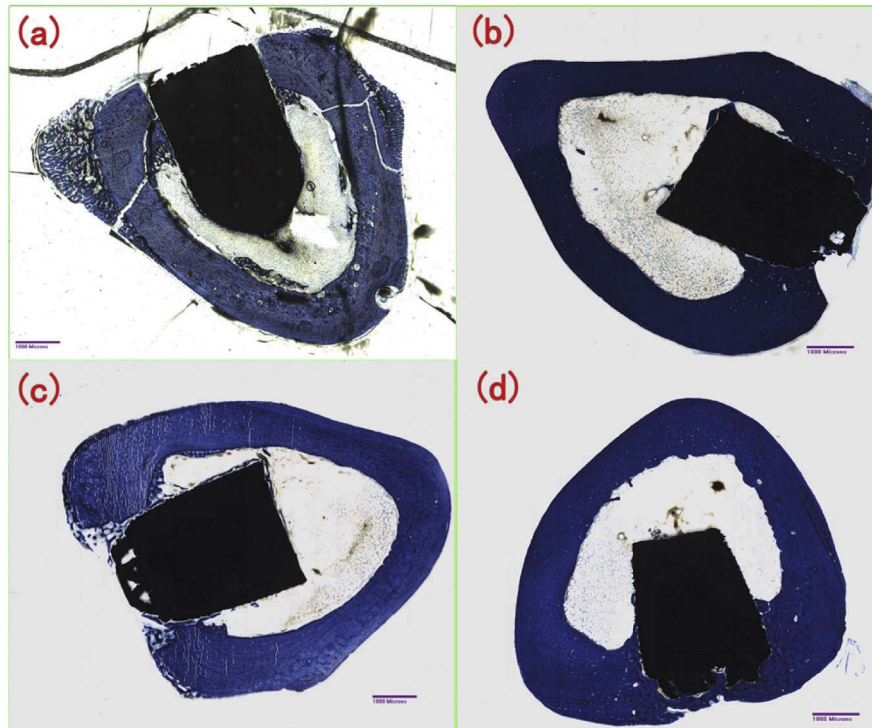


Fig. 7. Longitudinal cross-sections of the prepared implant cavities: (a) Experimental group at 4 weeks; (b) Experimental group at 8 weeks; (c) Control group at 4 weeks; (d) Control group at 8 weeks.

4. Discussion

Automated preparation of dental implant cavities using microrobots and femtosecond laser ablation is proposed in this pioneering work. Compared with the traditional method, the proposed method can improve the accuracy of implant surgery and the speed of osseointegration, shorten the time of implant surgery, and reduce the fatigue strength of dentists. The feasibility of this method was also preliminarily validated by *ex vivo* animal experiments.

The primary aim of this work was to determine how the depth-of-cut of femtosecond laser ablation could be precisely controlled along with the resulting bone tissue morphologies. An optimal set of parameters was derived for a single-pass depth-of-cut to facilitate precise implant cavity preparation. In a previous study, a three-axis robot-controlled picosecond laser was used for cortical-bone ablation [38]; however, the depth-of-cut of the picosecond laser was limited for the cortical bone, which is insufficient for dental implant surgery. In this work, the single-pass depth-of-cut of a femtosecond laser on bone tissue was measured via stepped laser cuts of concentric circles on rabbit femurs while varying the operational parameters (i.e., laser power, frequency, spot diameter, and scanning rate). The movements of the focal plane (i.e., movements of the laser lens) were configured according to the optimal depth-of-cut parameters such that the cutting plane was always located along the focal plane. Thus, our system could achieve the required depth-of-cut for dental implant surgery.

The effects of femtosecond laser ablation on bone tissues depend on parameters such as scanning rate and output power. A non-optimal set of parameters could increase the cavity taper, induce carbonization, and increase tissue temperature (5–100 °C). In our experiments, it was found, that when the scanning rate was unchanged, an increase in laser power increased

the depth-of-cut; however, this tended to induce carbonization on the surfaces of the osseous tissues. When the laser power was fixed, the depth-of-cut increased with decreasing scan rate. This trend is consistent with the variation of the single-point ablation rate with the laser power and the number of applied pulses. Because cutting is a superposition of single-point ablation, the power, corresponding energy density, single-point ablation rate, and the cutting depth will increase. However, an extremely high energy will be absorbed by the bone tissue and converted into heat, which can easily lead to the carbonization of the bone tissue. Reducing the scanning speed is equivalent to increasing the number of pulses of a single-point action; accordingly, the single-point ablation rate and cutting depth will increase. Thus, the *ex vivo* animal bone experiments allowed the determination of the optimal parameters for automated implant cavity preparation and proved the feasibility of the method using robot-controlled femtosecond laser ablation. The findings of these experiments also serve as the basis for live animal experiments.

In the live animal experiments, it was observed that the proposed method had positive effects on osteogenic activity. It has previously been shown that femtosecond laser ablation of the cortical bone could promote the osteogenic differentiation of the BMSCs [39]. In view of this finding, we performed western blot analysis to measure the expressions of osteogenic proteins by the BMSCs in an osteoinductive environment after seven days using femur samples subjected to the automated implant cavity preparation approach. The BICs of the titanium implants in these cavities were also measured to confirm the osseointegration effects of femtosecond laser ablation.

5. Conclusions

To address the limitations of the current traditional methods of preparing oral implant cavities, we presented a robotically controlled femtosecond laser ablation method for automated implant cavity preparation, along with a preliminary validation of this method. The results demonstrate that implant cavity preparation via femtosecond laser ablation promotes osseointegration to a certain extent. However, because this approach is still in its early stages of development, it is yet to be systematically validated; furthermore, a few issues associated with this method need to be resolved. In future research, we will further optimize the appropriate parameters for the automatic preparation of the implant site, improve the quality and efficiency of automated implant surgery, and further study the mechanism of femtosecond-laser-induced osteogenesis, which will help establish a solid foundation for clinical applications.

Funding. National Key Research and Development Program of China (2020YFB1312801); the Opening Research Fund of the State Key Laboratory for Advanced Metals and Materials (2021-Z08); National Natural Science Foundation of China (81571023).

Acknowledgments. We sincerely thank our doctoral supervisor, Prof. Lyu Peijun, a pioneer in the field of robot-controlled femtosecond lasers for oral surgery, who proposed a new concept for robot-controlled femtosecond-laser-automated implant preparation.

Disclosures. The authors declare no conflicts of interest.

Author Contributions: Conceptualization, F.S.Y.; methodology, S.S.L and J.Q.Z.; formal analysis, S.S.L.; writing—original draft preparation, F.S.Y and S.S.L.; writing—review and editing, F.S.Y. All authors read and approved the final manuscript.

Data availability. Data underlying the results presented in this paper are not publicly available at this time but may be obtained from the authors upon reasonable request.

References

1. D. Buser, L. Sennerby, and H. De Bruyn, "Modern implant dentistry based on osseointegration: 50 years of progress, current trends and open questions," *Periodontol* **2000** *73*(1), 7–21 (2017).
2. J. Chen, M. Cai, J. Yang, T. Aldhohrah, and Y. Wang, "Immediate versus early or conventional loading dental implants with fixed prostheses: A systematic review and meta-analysis of randomized controlled clinical trials," *The Journal of Prosthetic Dentistry* **122**(6), 516–536 (2019).
3. J. Hartlev, P. Kohberg, S. Ahlmann, N.T. Andersen, S. Schou, and F. Isidor, "Patient satisfaction and esthetic outcome after immediate placement and provisionalization of single-tooth implants involving a definitive individual abutment," *Clin. Oral Impl. Res.* **25**(11), 1245–1250 (2014).

4. H.W. Elani, J.R. Starr, J.D. Da Silva, and G.O. Gallucci, "Trends in Dental Implant Use in the U.S., 1999-2016, and Projections to 2026," *J. Dent. Res.* **97**(13), 1424–1430 (2018).
5. H.L. Feng and J. Xu, *Prosthodontics* (Peking University Medical Publication, 2012), Chap. 2.
6. B.D. Kennedy, T.A. Collins Jr., and P.C. Kline, "Simplified guide for precise implant placement: a technical note," *Int. J. Oral Maxillofac. Implants* **13**(5), 684–688 (1998).
7. S.L. Oh, H.J. Shiau, and M.A. Reynolds, "Survival of dental implants at sites after implant failure: A systematic review," *J. Prosthet Dent.* **123**(1), 54–60 (2020).
8. S.H. Park and H.L. Wang, "Implant reversible complications: classification and treatments," *Implant Dent.* **14**(3), 211–220 (2005).
9. R. Jacobs, M. Quirynen, and M.M. Bornstein, "Neurovascular disturbances after implant surgery," *Periodontol 2000* **66**(1), 188–202 (2014).
10. S. Longoni, M. Sartori, M. Braun, P. Bravetti, A. Lapi, M. Baldoni, and G. Tredici, "Lingual vascular canals of the mandible: The risk of bleeding complications during implant procedures," *Implant Dent.* **16**(2), 131–138 (2007).
11. J. D'haese, J. Ackhurst, D. Wismeijer, H. De Bruyn, and A. Tahmaseb, "Current state of the art of computer-guided implant surgery," *Periodontol 2000* **73**(1), 121–133 (2017).
12. K.C. Oh, J.M. Park, J.S. Shim, J.H. Kim, J.E. Kim, and J.H. Kim, "Assessment of metal sleeve-free 3D-printed implant surgical guides," *Dent. Mater.* **35**(3), 468–476 (2019).
13. C.C. Lin, C.Z. Wu, M.S. Huang, C.F. Huang, H.C. Cheng, and D.P. Wang, "Fully digital workflow for planning static guided implant surgery: a prospective accuracy study," *J. Clin. Med.* **9**(4), 980 (2020).
14. G. A. Mediavilla, D. E. Riad, Á. Zubizarreta-Macho, R. Agustín-Panadero, and M. S. Hernández, "Accuracy of computer-aided dynamic navigation compared to computer-aided static navigation for dental implant placement: an in vitro study," *J. Clin. Med.* **8**(12), 2123 (2019).
15. J. Gargallo-Albiol, S. Barootchi, O. Salomó-Coll, and H.L. Wang, "Advantages and disadvantages of implant navigation surgery. a systematic review," *Annals of Anatomy - Anatomischer Anzeiger* **225**, 1–10 (2019).
16. G. Maza and A. Sharma, "Past, present, and future of robotic surgery," *Otolaryngologic Clinics of North America* **53**(6), 935–941 (2020).
17. Y. Wu, F. Wang, S. Fan, and J. K. Chow, "Robotics in dental implantology," *Oral and Maxillofacial Surgery Clinics of North America* **31**(3), 513–518 (2019).
18. K.J. Cheng, T.S. Kan, Y.F. Liu, W.D. Zhu, F.D. Zhu, W.B. Wang, X.F. Jiang, and X.T. Dong, "Accuracy of dental implant surgery with robotic position feedback and registration algorithm: an in-vitro study," *Comput. Biol. Med.* **129**, 104153 (2021).
19. S.L. Bolding and U.N. Reebye, "Accuracy of haptic robotic guidance of dental implant surgery for completely edentulous arches," *The Journal of Prosthetic Dentistry* **26**, 500 (2021).
20. F.S. Yuan, J.Q. Zheng, Y.P. Zhang, Y. Wang, Y.C. Sun, and P.J. Lyu, "Preliminary study on the automatic preparation of dental implant socket controlled by micro-robot," *Zhonghua Kou Qiang Yi Xue Za Zhi* **53**(8), 524–528 (2018).
21. T. Albrektsson and A. Eriksson, "Letters to the Editor," *Clin. Orthop. Relat. Res.* **311** (1985).
22. D.L. Brisman, "The effect of speed, pressure, and time on bone temperature during the drilling of implant sites," *Int. J. Oral Maxil. Implants* **11**(1), 35–37 (1996).
23. C. Ercoli, P.D. Funkenbusch, H.J. Lee, M.E. Moss, and G.N. Graser, "The influence of drill wear on cutting efficiency and heat production during osteotomy preparation for dental implants: a study of drill durability," *Int. J. Oral Maxil. Implants* **19**(3), 335–349 (2004).
24. G.E. Chacon, D.L. Bower, P.E. Larsen, E.A. McGlumphy, and F.M. Beck, "Heat production by 3 implant drill systems after repeated drilling and sterilization," *Journal of Oral and Maxillofacial Surgery* **64**(2), 265–269 (2006).
25. A. Vogel and V. Venugopalan, "Mechanisms of pulsed laser ablation of biological tissues," *Chem. Rev.* **103**(2), 577–644 (2003).
26. C. Kerse, H. Kalaycıoğlu, P. Elahi, B. Çetin, D.K. Kesim, Ö. Akçaalan, S. Yavaş, M.D. Aşık, B. Öktem, H. Hoogland, R. Holzwarth, and F.Ö. Ilday, "Ablation-cooled material removal with ultrafast bursts of pulses," *Nature* **537**(7618), 84–88 (2016).
27. H. He, S.Y. Li, S.Y. Wang, M.L. Hu, Y.J. Cao, and C.Y. Wang, "Manipulation of cellular light from green fluorescent protein by a femtosecond laser," *Nature Photon* **6**(10), 651–656 (2012).
28. P. Cheng, X.Y. Tian, W.Y. Tang, J. Cheng, J. Bao, H.P. Wang, S.S. Zheng, Y.J. Wang, X.B. Wei, T.N. Chen, H. Feng, T. Xue, K. Goda, and H. He, "Direct control of store-operated calcium channels by ultrafast laser," *Cell Res.* **31**(7), 758–772 (2021).
29. C. Schweitzer, A. Brezin, B. Cochener, D. Monnet, C. Germain, S. Roseng, R. Sitta, A. Maillard, N. Hayes, P. Denis, P.J. Pisella, and A. Benard, "Femtosecond laser-assisted versus phacoemulsification cataract surgery (FEMCAT): a multicentre participant-masked randomised superiority and cost-effectiveness trial," *Lancet* **395**(10219), 212–224 (2020).
30. T.I. Kim, J.L. Alió Del Barrio, M. Wilkins, B. Cochener, and M. Ang, "Refractive surgery," *Lancet* **393**(10185), 2085–2098 (2019).
31. M. Malinauskas, A. Žukauskas, S. Hasegawa, Y. Hayasaki, V. Mizeikis, R. Buividas, and S. Juodkazis, "Ultrafast laser processing of materials: from science to industry," *Light Sci Appl* **5**(8), e16133 (2016).
32. J. Zhang, K. Guan, Z. Zhang, and Y. Guan, "In vitro evaluation of ultrafast laser drilling large-size holes on sheepshank bone," *Opt. Express* **28**(17), 25528–25544 (2020).

33. L.J. Mortensen, C. Alt, R. Turcotte, M. Masek, T.M. Liu, D.C. Côté, C. Xu, G. Intini, and C.P. Lin, "Femtosecond laser bone ablation with a high repetition rate fiber laser source," *Biomed. Opt. Express* **6**(1), 32–42 (2015).
34. Y.C. Lim, K.J. Altman, D.F. Farson, and K.M. Flores, "Micropillar fabrication on bovine cortical bone by direct-write femtosecond laser ablation," *J. Biomed. Opt.* **14**(6), 064021 (2009).
35. R.G. McCaughey, H. Sun, V.S. Rothholtz, T. Juhasz, and B.J. Wong, "Femtosecond laser ablation of the stapes," *J. Biomed. Opt.* **14**(2), 024040 (2009).
36. D.D. Lo, M.A. Mackanos, M.T. Chung, J.S. Hyun, D.T. Montoro, M. Grova, C. Liu, J. Wang, D. Palanker, A.J. Connolly, M.T. Longaker, C. H. Contag, and D. C. Wan, "Femtosecond plasma mediated laser ablation has advantages over mechanical osteotomy of cranial bone," *Lasers Surg. Med.* **44**(10), 805–814 (2012).
37. E. Su, H. Sun, T. Juhasz, and B.J. Wong, "Preclinical investigations of articular cartilage ablation with femtosecond and pulsed infrared lasers as an alternative to microfracture surgery," *J. Biomed. Opt.* **19**(9), 098001 (2014).
38. S. Liang, P. Lyu, and F. Yuan, "Method for accurately preparing cavities on cortical bones using picosecond laser," *Photobiomodulation, Photomedicine, and Laser Surgery* **38**(5), 301–307 (2020).
39. J. Zheng, X. Zhang, Y. Zhang, and F. Yuan, "Osteoblast Differentiation of bone marrow stromal cells by femtosecond laser bone ablation," *Biomed. Opt. Express* **11**(2), 885–894 (2020).